

# Modulation Crack Growth and Crack Coalescence upon Langmuir Monolayer Collapse

E. Hatta\* and Th. M. Fischer

Max Planck Institute of Colloids and Interfaces, Am Mühlenberg 1, 14476 Golm, Germany

Received: May 1, 2001; In Final Form: September 24, 2001

An extensive study for Langmuir monolayer collapse is carried out to explore the generality of classification of their crack patterns (E. Hatta et al. *Eur. Phys. J.* **1999**, B11, 609) and to analyze crack kinetics in the anisotropic cracks. Upon compression of fatty acid monolayers beyond the collapse pressure three classes of fracture patterns, a surface roughening, random crack network, or anisotropic fracture, can be observed depending on chain length of the fatty acid, pH value, and ion concentration of the subphase. A statistical characterization of the anisotropic crack growth of Langmuir monolayer fracture is presented. Anisotropic cracks grow on a  $\text{Co}^{2+}$  water subphase as quasi-periodic modulations, branching off previously formed cracks, interrupted by the coalescence of modulation cracks. Slight changes in pH and concentration of  $\text{Co}^{2+}$  ions in the subphase cause drastic changes of the modulation crack coalescence rate. We suggest, that differences in the viscoelastic nature of the monolayer are the main causes for the three types of crack growth scenaria.

In soft condensed matter already moderate external stress may lead to nonlinear response of the material. Spontaneous and strongly correlated, dynamic collective behavior originating in the internal degrees of freedom of the constituent molecules give rise to a rich variety of nonlinear physical and chemical effects.<sup>1</sup> Fracture of soft condensed matter such as gels,<sup>2</sup> vesicles,<sup>3</sup> colloidal suspensions,<sup>4</sup> Langmuir monolayers,<sup>5–9</sup> and foams<sup>10</sup> result in various fracture patterns and spatio temporal characteristics.

Different material properties in ordered and disordered matter govern the formation,<sup>11</sup> evolution,<sup>12</sup> and coalescence<sup>13</sup> of cracks. In solids, the simplest model is that of the competition of stress release versus the creation of surface energy (Griffith criterion<sup>11</sup>), which governs the formation of a crack. It usually works well, because the region of large deformation and hence nonlinear stress–strain relationship is restricted to a small area near the tip of the crack. In soft condensed matter large deformation can exist in a macroscopic region ranging far away from the tip. It is therefore not surprising to observe new types of crack growth unexplored in solid-state materials. As the nonlinear material parameters in the constitutive equations become more important, there are several ways in which a system can change its dynamical behavior. One of the major experimental problems in following the crack dynamics arises due to the time scale on which cracking occurs in solid-state material. Usually, a crack alternates between rapid motion and arrest, and it is difficult to resolve the evolution of a crack growth. We will show that promising systems to overcome such problems are Langmuir monolayers.<sup>14</sup> Langmuir monolayers may crack, when compressed beyond the collapse pressure, where the two-dimensional arrangement of molecules at the air/water interface becomes unstable and the molecules start to explore the third dimension. Different phases, with drastic changes in mechanical properties, can be easily prepared by varying the density, temperature, and subphase composition. A particularly interesting effect occurs when adding divalent ions to the subphase, which increase the surface shear viscosity of the monolayer<sup>15</sup> and slow the dynamics. Indeed, in our previous experiments,<sup>6</sup> it was observed

that the morphology of collapsed Langmuir monolayers from isotropic random network to anisotropic crack alignment undergoes a first-order transition, with increasing pH value and in the presence of specific ions (i.e.,  $\text{Co}^{2+}$ ). This change was accompanied by the slowing down of crack velocity. These observations, however, were focused on stearic acid in the presence of  $\text{Co}^{2+}$  ions and the generality of the classification of crack patterns for other fatty acids and in the presence of other divalent ions and the detailed analysis of crack kinetics in the anisotropic case were unexplored. Here, we report on an extensive study of the crack growth and crack formation in Langmuir monolayers steadily compressed beyond the collapse pressure and demonstrate the validity of the previously described classification scheme of crack patterns. As for the crack kinetics in the anisotropic crack growth a quantitative statistical analysis is given and the sensitivity of the crack coalescence rates on pH and  $\text{Co}^{2+}$  concentration is shown.

## Experimental Section

Monolayers of fatty acids [stearic acid (octadecanoic acid), arachidic acid (eicosanoic acid), and lignoceric acid (tetra-cosanoic acid), 99% pure, Sigma Chemicals] dissolved in *n*-hexane (99% pure, Kanto Chemicals) 0.5 mmol were spread onto a subphase (Millipore Mill-Q system filtered water, 18.0 MΩ cm) containing 1.0–2.0 mMol of salt ( $\text{CoCl}_2$ ,  $\text{CdCl}_2$ ,  $\text{MnCl}_2$ , or  $\text{BaCl}_2$  Rare Metallic, purity 99.999%) at  $20.0 \pm 0.2$  °C. The pH value of the subphase was adjusted in the range 6–7.8 with  $\text{NaHCO}_3$ . All materials were used without further purification. The monolayers were compressed to the super liquid LS-phase and beyond the collapse pressure  $\pi_c$  with a fixed rate  $\dot{A} = -1.66 \cdot 10^{-5} \text{ m}^2/\text{s}$  using a barrier. The pressure during that compression remained constant slightly above the collapse pressure, thereby forcing the molecules into the third dimension at a rate  $\dot{N}_3 = -N_2 \dot{A}/A$ , where  $N_3$  is the total number of molecules forced into the third dimension and  $N_2$  is the number of molecules remaining in a two-dimensional arrangement of the interface. Cracks in the monolayer were monitored via three-dimensional aggregates protruding from the cracks using phase contrast microscopy (NIKON, OPTIPHOT-2) equipped with a

\* Corresponding author. E-mail: eiji.hatta@mpikg-golm.mpg.de.

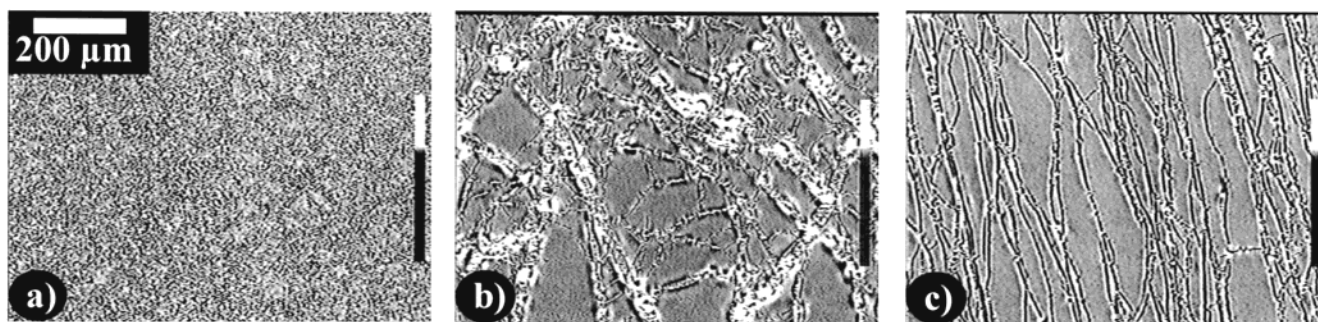


**Figure 1.** Phase contrast microscopy images of three different types of crack patterns in Langmuir monolayers beyond the collapse pressures. A surface roughening crack pattern (stearic acid, pH = 7.0, (a)), a random crack network (arachidic acid + 1 mMol Cd<sup>2+</sup>, pH = 7.8, (b)), and an anisotropic crack alignment (stearic acid + 1 mMol Co<sup>2+</sup>, pH = 7.5, (c)).

**TABLE 1: A Classification of the Crack Patterns in Langmuir Monolayers under Various Conditions**

	random network			anisotropic fracture			surface roughening		
	pH	ion	<i>c</i> [mMol]	pH	ion	<i>c</i> [mMol]	pH	ion	<i>c</i> [mMol]
stearic acid	7.8						6–7.5		
	6	Co <sup>2+</sup>	1–2	7–7.8	Co <sup>2+</sup>	1–2			
	6–7.8	Cd <sup>2+</sup>	1						
	7–7.8	Mn <sup>2+</sup>	1				6	Mn <sup>2+</sup>	1
arachidic acid	6–7.5	Ba <sup>2+</sup>	1						
							6–7.8		
	6	Co <sup>2+</sup>	1	7–7.8	Co <sup>2+</sup>	1			
lignoceric acid	6–7.8	Cd <sup>2+</sup>	1				6–7.8	Mn <sup>2+</sup>	1
							6–7.8		
							6–7.5	Cd <sup>2+</sup>	1

CCD camera (Hamamatsu, C2400-77H) followed by an image processor (Hamamatsu DVS-3000).<sup>16</sup> Phase contrast microscopy is insensitive to the 2d-monoayer and the intensity of the image is proportional to the amount of protruded molecules  $N_3$ . The crack formation, evolution, and coalescence was videotaped with frequency (30 frames/s) while constantly monitoring the monolayer area *A* and surface pressure  $\pi$ . The monolayer was also visualized with Brewster angle microscopy (BAM)<sup>17,18</sup> using an Ar-ion laser operated at  $\lambda = 514$  nm and  $P = 350$  mW.

## Results

A steady compression increases the monolayer pressure until a pressure slightly above  $\pi_c$  is reached. Then the pressure remains constant and cracks are formed. The crack pattern depends on the amphiphilic molecule, the pH-value of the subphase, and the subphase ion-concentration. We have performed room-temperature experiments ( $T = 20$  °C) with stearic, arachidic, and lignoceric acid on pure water of pH = 6.0–7.8 (using NaHCO<sub>3</sub>) and on water containing Ba<sup>2+</sup>, Cd<sup>2+</sup>, Mn<sup>2+</sup>, Co<sup>2+</sup>. The crack patterns observed can be divided into three classes (Figure 1): a surface roughening pattern, where cracks are at the resolution limit (0.5  $\mu$ m) of the microscope and the crack pattern resembles a granular structure (Figure 1a); a random crack network (Figure 1b), where cracks grow in arbitrary directions; and a well-oriented anisotropic assembly of aligned cracks (Figure 1c) growing approximately perpendicular (from the top toward the bottom) to the compression direction (from the left toward the right). The kinetics of crack growth for the surface roughening and random network cracking occurs very fast and cannot be resolved with video frequency resolution. The anisotropic fracture, however, is significantly slower and we will focus on the anisotropic crack growth kinetics in the second part of the paper. A classification scheme of the crack patterns observed under various conditions is shown in Table 1. Most of the fatty acids crack in a random network

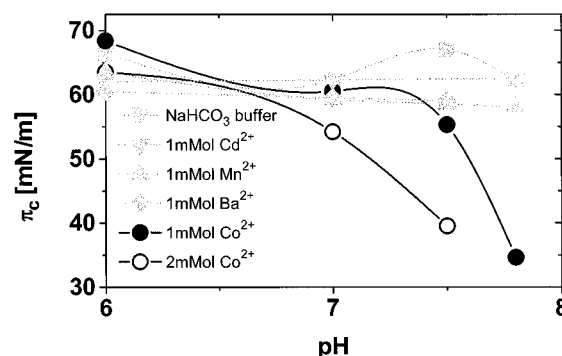


**Figure 2.** Collapse pressure ( $\pi_c$ )–pH value characteristics in stearic acid monolayers with different ions. Note that a significant decrease of the collapse pressure is observed with pH values only in the presence of Co<sup>2+</sup> ions.

fashion. Surface roughening is observed on pure water and in the presence of Mn<sup>2+</sup> or Cd<sup>2+</sup>. Anisotropic fracture is rare and only occurred in the presence of Co<sup>2+</sup> ions. Obviously Co<sup>2+</sup> ions must bind in a specific way to the amphiphiles, thereby causing special mechanical properties of the monolayer. The different collapse behavior of the monolayer can already be found in the collapse pressure (Figure 2). While for Ba<sup>2+</sup>, Cd<sup>2+</sup>, Mn<sup>2+</sup> ions the collapse pressure is more or less independent of the pH-value of the subphase; a significant decrease of the collapse pressure with pH is observed in the presence of Co<sup>2+</sup> ions.

In Figure 3 we show the typical crack line pattern kinetics in a stearic acid monolayer ( $\pi_c = 55.3$  mN/m) on a pH = 7.5, 1 mmol Co<sup>2+</sup> water subphase. Crack lines follow a path approximately perpendicular to the compression direction (from left to right). If we assume that only one of the cracks grows at a time we can estimate the speed of the front to be  $v = \dot{A}d/\sigma \approx 10^{-2}$

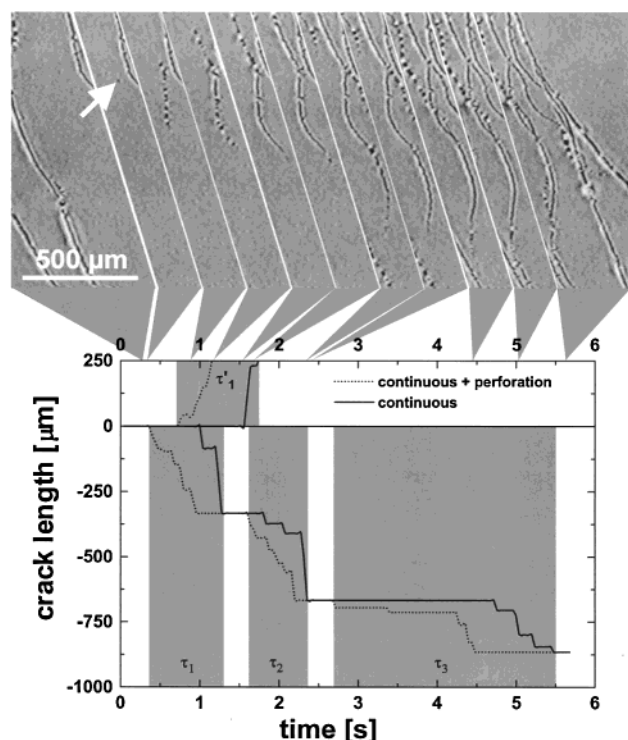


**Figure 3.** Phase contrast microscopy images of the evolution of a crack line in a stearic acid monolayer in the presence of 1 mMol  $\text{Co}^{2+}$  ions and at pH = 7.5. The crack nucleates close to another crack (white arrow) and propagates by forming a modulation crack. Then the modulation coalesces and the process repeats. The continuous crack length (solid line) and the continuous plus modulated crack length (dotted line) of this crack is plotted versus time in the lower graph. The length of each modulation period is marked in gray. Most of the time the crack is in a modulated state. The modulation state is interrupted by crack coalescence events occurring with a rate of  $\Gamma = 0.95 \text{ s}^{-1}$ .

m/s, where  $d \approx 2 \text{ nm}$  is the thickness of the monolayer and  $\sigma \approx 10^{-12} \text{ m}^2$  the cross section of a crack. The observed front velocity was somewhat lower,  $10^{-3}$ – $10^{-4} \text{ m/s}$ . As is clear below, however, we see that the front speed can be changed by the order of magnitude easily even at a fixed compression rate with adjustable parameters (i.e., pH and  $\text{Co}^{2+}$  concentration). The crack front speed could be higher (or lower) under a certain condition. The cracking mechanism observed is thus found to be more complicated than the above-described mechanism, presumably because of more than one crack growth at a time. In this figure we can see the alternative crack growth of dot-like crack nucleation and its coalescence. It is not clear at present that the observed “dots” are indeed isolated holes or valleys. They could be connected structures of bent or twisted monolayers. We thus call the crack evolution observed as “modulation” crack below.

In Figure 3, a virgin modulation crack marked by an arrow nucleates in front of a long continuous crack. The evolution of this particular crack is followed as a function of time in the consecutive images in Figure 3. We can see that most of the time the crack consists of a modulated front, interrupted by short events, when the modulation cracks coalesce to form one continuous crack from the rear to the front. After the coalescence new modulations evolve in front of the crack in this way propagating the crack further into the undisturbed monolayer region. Then the scenario is repeated, however, the time lag  $\tau$  between the onset of the modulation growth and its coalescence varies from one cycle to the next. For the crack shown in Figure 3 we have plotted the length of the continuous part of the crack

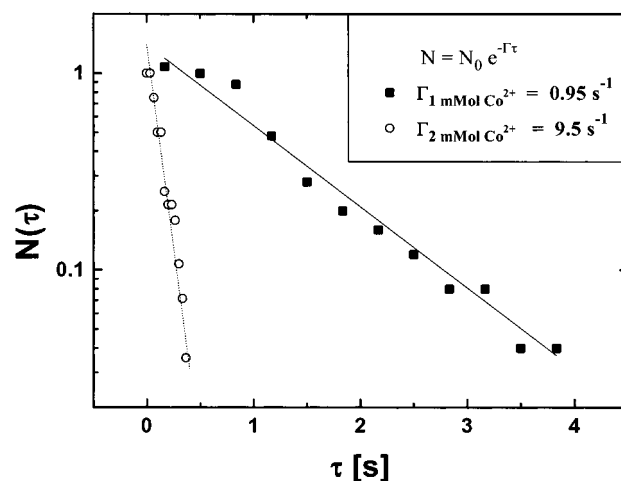


**Figure 4.** The cumulative distribution of individual lifetimes of the modulated cracks in the stearic acid monolayer in the presence of 1 mMol (a) and 2 mMol (b)  $\text{Co}^{2+}$  ions and at pH = 7.5. Both distributions exponentially decay with  $\tau$ . Note that the exponential decay rate  $\Gamma$  is very sensitive to changes in the  $\text{Co}^{2+}$  concentration.

(solid line) as well as the length of the whole crack (continuous plus modulated section, dotted line) as a function of time. The time intervals  $\tau$  where both lengths are different are marked in gray. The cumulative distribution of individual lifetimes  $\tau$  of the modulated sections  $N(\tau) = M(\tau)/M(0)$  is presented in Figure 4.  $M(\tau)$  is the number of modulated crack growth events lasting at least for a time  $\tau$  before the modulated cracks coalesce. The data are taken from  $M(0) = 200$  events accumulated from 40 different cracks, locations, and times. The distribution exponentially decreases with  $\tau$  with a rate  $\Gamma = (0.95 \pm 0.03) \text{ s}^{-1}$ . Doubling the ion concentration while keeping all the other conditions fixed, speeds up this process by a factor of 10. In Figure 5 a typical crack growth is shown for 2 mMol  $\text{Co}^{2+}$  ion concentration. Here the cracks are usually straighter compared to 1 mMol  $\text{Co}^{2+}$ . Modulated crack growth and coalescence happens within a few frames. A plot of the cumulative distribution of modulation crack lifetimes again yields an exponential decay with a rate of  $\Gamma = (9.5 \pm 0.5) \text{ s}^{-1}$ .

A Brewster angle microscope (BAM) image of a modulation crack is shown in Figure 6. The pH value of subphase is somewhat lower (pH = 7.3), compared to that of Figure 3. The monolayer visualized with BAM is in focus only in a very narrow region and we have difficulty with analyzing coalescence events in modulation crack evolutions statistically. However, it is seen easily qualitatively that the crack coalescence rate is higher than at pH = 7.5. In our previous experiments,<sup>6</sup> the coalescence events could not be seen any more in the monolayer at pH = 7.0. These results suggest that the modulation lifetime strongly depends on pH as well as  $\text{Co}^{2+}$  concentration. The high sensitivity of modulation crack coalescence events on pH and  $\text{Co}^{2+}$  concentrations means that Langmuir monolayers provide one of the few system where crack events can be controlled artificially.<sup>19</sup>

The strong dependency of the modulation crack lifetime and collapse pressure on  $\text{Co}^{2+}$  concentration suggests a drastic change in mechanical properties of the monolayer. One guess is that  $\text{Co}^{2+}$  ions might change the thermodynamic phase of the acids if the pH is high enough. The phase behavior of fatty acids has been subject of intense studies.<sup>14</sup> Most of the recent work, based on grazing incidence X-ray diffraction data suggests that the acids are in the LS-phase, where molecules are in an upright undistorted hexatic order and free to rotate around their long axis. However, the early work of Stållberg-Stenhagen and



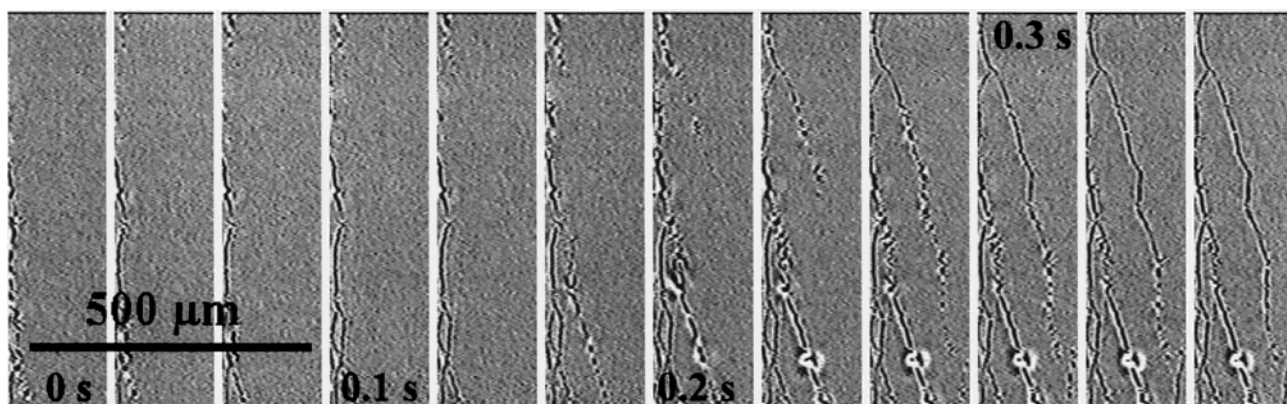


**Figure 5.** Phase contrast microscopy images of a typical crack evolution in the stearic acid monolayer in the presence of 2 mMol  $\text{Co}^{2+}$  ions and at pH = 7.5. The duration of the sequence of modulation crack and coalescence becomes much shorter than at 1 mMol  $\text{Co}^{2+}$  concentration.

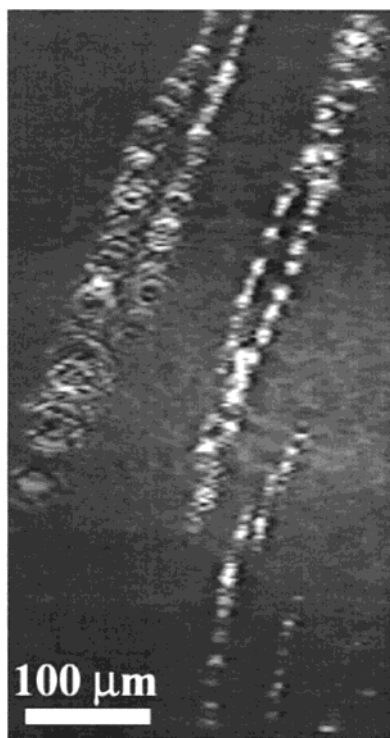


**Figure 6.** Brewster angle microscope image of an anisotropic crack in stearic acid monolayer in the presence of 1 mMol  $\text{Co}^{2+}$  ions and at pH = 7.3. Under these conditions the duration of the sequence of modulation crack and coalescence becomes much shorter than at pH = 7.5.

Stenhagen<sup>20</sup> showed, that in behenic acid at pressure values above 40 mN/m the S phase invades temperature regions 30 K higher than where it is usually observed at lower ( $\pi = 30$  mN/m) surface pressures and where most of the X-ray work was done. It could be that depending on the  $\text{Co}^{2+}$  concentration and the pH value the collapse pressure is lowered such that this invasion does not occur, suggesting that the random network cracking occurs in the S-phase and the anisotropic cracking in the LS-phase. If this hypothesis were correct it is easy to understand the directions of the cracks. If the phase itself is anisotropic as in the S-phase, cracks will grow along arbitrarily oriented grain boundaries or easy axes of the arbitrarily oriented grains and form a random crack network. If however the phase is 2d-isotropic like the LS-phase, than preferred crack directions are imposed by the anisotropic compression of the barrier and cracks grow perpendicular to the compression direction. A clear picture, however, of what goes on relies on further X-ray data close to the collapse region.

## Conclusions

Three different types of Langmuir monolayer cracking upon collapse have been observed. Monolayer collapse either occurs as random network cracking, anisotropic fracture, or surface roughening in various fatty acids and in the presence of divalent ions. The anisotropic fracture consists of modulated cracks growing perpendicular to the compression direction and only coalescing after a certain time. The lifetime of modulated cracks strongly depends on pH and  $\text{Co}^{2+}$  concentration. The modulated crack growth seems to be correlated with a special effect occurring only in the presence of  $\text{Co}^{2+}$  ions. Presumably there might be an effect of  $\text{Co}^{2+}$  ions on the phase behavior.

**Acknowledgment.** We thank Prof. H. Möhwald for generous support and stimulating discussion. E. Hatta thanks the Max-Planck-Gesellschaft for providing a Max-Planck fellowship. T. Fischer thanks the Deutsche Forschungsgemeinschaft for providing a Heisenberg fellowship.

## References and Notes

- (1) Witten, T. A. *Rev. Mod. Phys.* **1999**, *71*, S367.
- (2) Liu, C.-H.; Pine, D. J. *Phys. Rev. Lett.* **1996**, *77*, 2121.
- (3) Bar-Ziv, R.; Frisch, T.; Moses, E. *Phys. Rev. Lett.* **1995**, *75*, 3481.
- (4) Pauchard, L.; Parisse, F.; Allain, C. *Phys. Rev.* **1999**, *E59*, 3737.
- (5) Hatta, E.; Hosoi, H.; Akiyama, H.; Ishii, T.; Mukasa, K. *Eur. Phys. J.* **1998**, *B2*, 347.
- (6) Hatta, E.; Suzuki, D.; Nagao, J. *Eur. Phys. J.* **1999**, *B11*, 609.
- (7) Pauchard, L.; Meunier, J. *Phys. Rev. Lett.* **1993**, *70*, 3565.
- (8) Bonn, D.; Pauchard, L.; Shahidzadeh, N.; Meunier, J. *Physica* **1999**, *A263*, 78.
- (9) Buzin, A. I.; Godovsky, Yu. K.; Makarova, N. N.; Fang, J.; Wang, X.; Knobler, C. M. *J. Phys. Chem. B* **1999**, *103*, 11372.
- (10) Müller, W.; di Meglio, J.-M. *J. Phys. Condens. Matter* **1999**, *11*, L209.
- (11) Griffith, A. A. *Philos. Trans. R. Soc. London, Sec. A* **1921**, 221, 163.
- (12) Fineberg, J.; Gross, S. P.; Marder, M.; Swinney, H. L. *Phys. Rev.* **1992**, *B45*, 5146.
- (13) Lu, C.; Vere-Jones, D.; Takayasu, H. *Phys. Rev. Lett.* **1999**, *82*, 347.
- (14) For reviews of Langmuir monolayers, see, Kaganer, V. M.; Möhwald, H. M.; Dutta, P. *Rev. Mod. Phys.* **1999**, *71*, 779.
- (15) Ghaskadvi, R. S.; Carr, S.; Dennin, M. *J. Chem. Phys.* **1999**, *111*, 3675.
- (16) Hosoi, H.; Akiyama, H.; Hatta, E.; Ishii, T.; Mukasa, K. *Jpn. J. Appl. Phys.* **1997**, *36*, 6927.
- (17) Hénon, S.; Meunier, J. *Rev. Sci. Instrum.* **1991**, *62*, 936.
- (18) Hönig, D.; Möbius, D. *J. Phys. Chem.* **1991**, *95*, 4590.
- (19) Yuse, A.; Sano, M. *Nature* **1993**, *362*, 329.
- (20) Stållberg-Stenhagen, S.; Stenhagen, E. *Nature* **1945**, *156*, 239.